Original Article

A universal mass-based index defining energy efficiency of different modes of passenger transport

Jing-Hua Zheng [a], Jianguo Lin [a, *], Julian M. Allwood [b], Trevor Dean [c]

[a] Department of Mechanical Engineering, Imperial College London, London SW7 2AZ, UK
[b] Engineering Department, University of Cambridge, Trumpington Street, Cambridge CB2 1PZ, UK
[c] Department of Mechanical Engineering, University of Birmingham, Edgbaston, Birmingham B15 2TT, UK

ARTICLE INFO

ABSTRACT

Reduction in vehicle weight can significantly reduce energy use in human transportation. However, to gauge efficiency, energy use and weight for a particular vehicle should be related to the number of people being transported while currently there is no convenient means to assess this. Here we statistically analyse the weight, energy consumption, carrying capacity and occupancy level for automobiles, buses, high-speed trains and aircraft. Based on the analysis and inspired by the medical body mass index (BMI), we have proposed a vehicle mass index (VMI), defined as $I = A\left(\frac{W_{tv}}{W_{tp}}\right)^{n}$, for the first time enables energy efficiency assessment of different transportations on a global scale, where n a weight sensitivity parameter and A the energy efficiency constant of a theoretically weightless vehicle. We show the VMI ranges and conclude the significant vehicle weight reduction windows to achieve their index lower limits. The possible limits for the VMI and the associated A and n values are also assessed. The concept of VMI could form the basis of a worldwide standard, useful in the current drive for a greener economy.
© 2021 The Authors. Publishing services by Elsevier B.V. on behalf of KeAi Communications Co. Ltd. This is an open access article under the CC BY-NC-ND license (http://creativecommons.org/licenses/by-nc-nd/4.0/).

Nomenclature

	Unit	Description
I	MJ/(person·km)	Vehicle Mass Index (VMI)
E_t	MJ/km	Total energy consumption for a vehicle travelling 1km
E_n	MJ/(person·km)	Normalized energy consumption (the total energy consumption normalized by carried passenger numbers for travelling 1km)
R	-	Normalized weight (total vehicle weight normalized by total passenger weight at a given occupancy level)
W_c, W_{tv}	kg	Vehicle curb weight and total vehicle weight (Vehicle curb weight + total passenger weight at a given occupancy level)
W_p, W_{tp}	kg	Individual passenger weight and total passenger weight in a vehicle at a given occupancy level

(continued)

	Unit	Description
N	-	Designed seat capacity of a vehicle
α	-	Vehicle seat occupancy level
A	MJ/(person·km)	Energy efficiency parameter for a theoretically weightless vehicle
n	-	Weight sensitivity parameter for a vehicle type
N_1, N_2	N	Vehicle vertical supporting forces on the left and right supporting wheels
C_S	-	Aerodynamic coefficient
ρ	kg/m^3	Air density
v_{wind}	m/s	Wind velocity
S	m^3	Vehicle crosswind projected area
μ	-	Friction coefficient
v	m/s	Vehicle velocity
r	m	Vehicle cornering radius
B	m	Width between two wheels of a vehicle
h	m	Height of the vehicle centroid
g	m/s^2	Gravity acceleration

* Corresponding author.
  E-mail address: Jianguo.lin@imperial.ac.uk (J. Lin).

1. Introduction

Growing concerns about escalating energy usage and CO_2 emissions require manufacturers of vehicles to find new ways to reduce their fuel consumption [1–3]. Reducing vehicle weight is one of the most effective ways to achieve this goal [4,5]. According to the weight reduction report, for high-speed rolling stock [6], aircraft [7] and automobiles [8], a 20% weight reduction could lead to about a 10%–16% increase in fuel efficiency [9–11]. For instance, modern-day aircraft, such as the Boeing 787, are 20% lighter than similar aircraft types due to the use of lightweight materials, and such weight savings results in fuel efficiency increases in the order of 10–12% [7]. Long-distance passenger trains could save 4% energy consumption for every 10% weight reduction and the energy savings could be 8% for subways and urban trains, according to the 2011 final report from IFEU ("Institute for Energy and Environmental Research") [12]. Similar benefits are also applied to automobiles. For example, 20% reductions in the gross weights of Finnish pre-Euro vehicles show a ~13% decrease in fuel consumptions when driving on freeflow rural roads. The fuel reductions could be up to ~16% when driving on saturated or urban roads [13]. For full electric vehicles, for example, the Tesla cars, the EPA driving range could extend from 220 miles to 280 miles with their vehicle-specific power (battery capacity/vehicle weight) increasing from 0.03 to 0.04 kWh/kg [14]. That translates to a 27% extension in the EPA driving range for a 25% reduction in vehicle weight, indicating the importance of weight reduction for electric cars. Provided with such substantial benefits from weight reductions, significant research is being performed to develop new technologies for manufacturing lightweight components at acceptable costs, for instance, HFQ® [15], double ram extrusion technology [16], multi-material light-weight gear forging [17].

Although manufacturing industry, in general, is devoted to accelerating the progress of light-weighting [18], there is no integrated analysis comparing the current status of weight, energy consumption and capacity for different types of transportation. More importantly, there is lacking any clearly defined vehicle mass index (VMI) to quantify weight levels from an energy efficiency perspective and to enable an integrated comparison between different transportation types. In coming decades, fossil fuel-derived energy will disappear to create a 'zero emissions' future, as has been already regulated for EU cars by 2035. However, green energy supply for the moment is less than hoped for. Reference to vehicle weight, energy consumption and carrying capacity can provide a useful indication of its efficiency and environmental impact, to enable a 'best choice' of transportation and hence a better and sustainable development.

Previous efforts have been made to evaluate trends of the vehicle energy consumptions and weight reductions for transportation [13,19,20]. Das et al. [21] predicted a cumulative energy saving of 6.1 billion GJ through light-weighting U.S. light-duty vehicles for 2017–2025. Official reports from the white paper [22] and transport paper [23] also confirmed an annual fuel burn reduced by 1.3% for commercial jet aircraft due to the use of lightweight materials. Attempts have been made to develop a cost-related or safety-based index. For example, Hofer, et al. [24] studied the effect of weight reduction on the energy use and cost of conventional vehicles and proposed cost-related formula for the determination of the optimum weight reduction for a minimized cost. Mayyas et al. [25] proposed a life cycle assessment based on lightweight design approach to assess the performance of automobile body-in-white. Lee et al. [26] developed an energy consumption formula as a function of flight parameters, including the weight of fuel, payload, seat, flight speed and lift to drag ratio, for aircraft. Metrics of fuel efficiency with respect to the maximum take-off weight has

also been developed by the International Civil Aviation Organizations [27] to gauge fuel use for different types of aircraft. Such metrics were further improved to rank the CO_2 intensity of commercial aircraft in proportion to emissions per seat kilometre flown for a single continuous line [28,29]. All the relevant work has made great contributions to the light-weight progress, building optimized design and evaluation methods for better reduction in energy consumptions and emissions. However, each publication has dealt with a specific transportation type whereas a universal vehicle mass index that enables comparison of all vehicle types is required to obtain an all-encompassing evaluation.

Probably the most well-known global index is the medical Body Mass Index (BMI) [30]. This is based on a person's height, weight and fatness and relates to large populations [30,31]. The pioneer of BWI is Adolphe Quetelet, who demonstrated that weight increases with the square of height and developed the well-known "Quetelet Index" ($Quetelet Index = \frac{Weight \, (kg)}{Height \, (m)^2}$). His index was ascribed no medical significance until 1972, when Ancel Keys (1904–2004) noticed that this 'normally-distributed' weight standard can be used to quantify an 'ideal' weight standard [32]. He showed that there is an approximately linear relationship between body fat percentage and the Quetelet Index, which was then renamed, 'Body Mass Index' (BMI). It is now widely used in routine physical examinations throughout the world.

Inspired by the BMI, in this paper, we integrate analysis of weight, energy consumption and passenger capacity for automobiles, buses, high-speed trains and aircraft. Normalising the data using passenger numbers enables a uniform comparison of these transportation modes. Based on this analysis, we define a unique physical-based vehicle mass index (VMI), I, which enables global assessment of the energy efficiency for all vehicle types for the first time. Ranges of VMI values for the analysed transportation types are presented together with estimates of the practically feasible minimum and maximum weights for automobiles and aircraft. The VMI could be widely applied to large populations of vehicles within each type for comparison and assessment of energy efficiency.

2. Weight per person and normalized energy of transportations

In this section, vehicle total weight per passenger carried, and the normalized energy (i.e. the energy used to carry a passenger for 1 km) for bus/coach, automobile, aircraft and high-speed train are presented. The vehicle total weight per carrying passenger is defined as

$$W_{tv} \Big/ (\alpha N) = \frac{W_c + \alpha N \cdot W_p}{\alpha N} \tag{1}$$

where W_{tv} is the vehicle total weight, including both the vehicle curb weight, W_c, and total passenger weight, W_{tp}. The total passenger weight is a product of the average passenger weight, W_p, and the carried passenger number, αN, where α is the average occupancy level of a vehicle and N the designed seat capacity. The normalized energy, E_n, is defined as

$$E_n = \frac{E_t}{\alpha N} \tag{2}$$

where E_t is the total energy consumption of a vehicle for travelling 1 km, αN is the number of passengers carried.

Fig. 1 presents the ranges and average values of total weight per person ($W_{tv}/(\alpha N)$) and normalized energy (E_n) for six transportation modes both at their current average seat occupancy levels

Fig. 1. Total weight per person ($W_{tv}/(\alpha N)$) and normalized energy (E_n) for six transportation modes at their average seat occupancy levels, α, (i.e. $\alpha = 1$, 1, 0.68, 0.32, 0.72 and 0.44 for walking, cycling, bus & coach, automobile, aircraft and high-speed train, respectively) and at their full seat capacity (i.e. $\alpha = 1$ for all types, and values are given in brackets).

($\alpha = 1$, 1, 0.68, 0.32, 0.72 and 0.44 [33] for walking, cycling, bus & coach, automobile, aircraft and high-speed train, respectively). The values in brackets are calculated based on the full (designed) seat capacity (i.e. $\alpha = 1$ for all transportation types). 'Ave' represents the average value calculated for each transport mode. The $W_{tv}/(\alpha N)$ value is derived assuming an average person weight, W_p, of 65 kg. Data and their sources are given in appendix A.

Considering the current average seat occupancy levels, walking and cycling, which require only human effort, have the lowest $W_{tv}/(\alpha N)$ values of 65 kg and 79 kg, respectively. For energy-driven transportations, bus/coach has the lowest $W_{tv}/(\alpha N)$ values, ranging from 309 to 640 kg/person with an average value of 516 kg/person. The $W_{tv}/(\alpha N)$ values are also low for aircraft with an average value of 633 kg/person. This may be due to both the high seat capacity and the

relatively high seat occupancy levels (0.68 for bus & coach and 0.72 for aircraft). The average $W_{tv}/(\alpha N)$ value for automobile is around 2 times higher (average 1141 kg/person) than those of bus&coach due to the low designed seat capacity and low seat occupancy level used by the passengers in real life. According to European Environment Agency (2015), the average seat usage is only 1.6 per automobile (occupancy level: 0.32). Hence the $W_{tv}/(\alpha N)$ values are high for automobiles compared to those of bus and aircraft. High-speed train is the 'heaviest' among these vehicles, ranging from 1727 to 3420 kg/person with an average $W_{tv}/(\alpha N)$ value of 2352 kg/person at the average occupancy level, which is around 2–4 times higher than those of other energy-driven transportation modes.

If the transportation vehicles are used at their full seat capacities, where the values are shown in brackets in Fig. 1 for $\alpha = 1$, the

$W_{tv}/(\alpha N)$ values reduce significantly for all energy-driven transportations. Bus&coach maintains the lowest $W_{tv}/(\alpha N)$ values among the four transportation types with the range of 210—435 kg/person and an average value of 351 kg/person. High-speed train retains the highest $W_{tv}/(\alpha N)$ values, ranging from 760 to 1505 kg/person, which is still 2—3 times higher than others and with an average value of 1035 kg/person. The largest change is the automobile, where their $W_{tv}/(\alpha N)$ values fall to 235—565 kg/person and become similar to bus& coach (i.e. 210-435 kg/person) and slightly lower than aircraft (i.e. 253-597 kg/person). This indicates the weight per passenger of the automobile could be comparable to that of public transportation if the seat capacity is fully occupied.

The values of normalized energy, E_n, for the vehicles are also shown in Fig. 1. At the current average seat occupancy levels, bus & coach (0.37 MJ/(person·km)) and high-speed train (0.45 MJ/(person·km)) have similar average values, and are the most energy-efficient ones with low normalized energies. The E_n value for automobile (i.e. 0.94 MJ/(person·km)) is around 2 times higher with a wide range of 0.31—2.53 MJ/(person·km) compared to high-speed train. The highest average E_n is the aircraft (1.39 MJ/(person·km)) though provided with a high seat occupancy level. A significant characteristic is the low energy consumption of high-speed train. Although, amongst the four modes, the $W_{tp}/(\alpha N)$ values of the high-speed train are highest, their E_n values are low.

When the vehicles are used at their full capacity, the average E_n values for bus, automobile and high-speed train become very low, only around 0.20—0.30 MJ/(person·km), while aircraft is still the most energy-consuming way for travelling with a high value E_n of 1.00 MJ/(person·km). It may be noted that the average E_n value of the aircraft at its full seat capacity (i.e. 1.00 MJ/(person·km)) is even higher than those of other transportation types at their current seat occupancy levels (i.e. 0.37 MJ/(person·km) for bus, 0.94 MJ/(person·km) for automobile, and 0.45 MJ/(person·km)) for high speed train. This implies that, from the energy consumption perspective, aircraft seems to be the least recommended transportation mode for travelling. However, considering its cruise speed (~900 km/h for aircraft), which is around 3 times higher than that of the high-speed trains (~300 km/h), 7—18 times higher than the automobiles (~50 km/h in city and ~120 km/h on highway) and 22 times higher than the buses (~40 km/h in city), aircraft is still very competitive, especially for long-distance journeys, although its energy efficiency is low.

Fig. 2a shows variations in $W_{tv}/(\alpha N)$ and E_n values for different transportation modes at their current average occupancy levels. $W_{tv}/(\alpha N)$ values for bus/coach and aircraft are the lowest among the four types of transportation modes. Overall, each person accounting for 309—829 kg of the total vehicle weight. A slight decrease in the $W_{tv}/(\alpha N)$ value occurs for bus&coach with the increase in seat capacity from 44 to 84. However, this trend does not apply to aircraft, where increasing seat capacity increases $W_{tv}/(\alpha N)$ values. Generally, long-haul aircraft (e.g. Airbus A330, Boeing 747, 787) have a larger capacity (e.g. 200—500) and fly at a haul distance of >4000 km while short-haul aircraft (e.g. Airbus A319, Boeing 737) have a smaller capacity (e.g. 89—300) and fly at a haul distance of ≤1500 km. The collected data shows that an increase in seat capacity with haul distance requires heavier aircraft and higher $W_{tv}/(\alpha N)$ values. Automobiles have a relatively fixed seat capacity of 5 and high $W_{tv}/(\alpha N)$ values in the range of 734—1765 kg/person. Such relative dispersed distribution includes small passenger cars and SUVs. The $W_{tv}/(\alpha N)$ values are extremely high for high-speed trains. They also vary greatly in the range 1727—3420 kg/passenger due to the different functions: only seats on day trains and beds on night trains which results in higher $W_{tv}/(\alpha N)$ values, as for the Zefiro 250 sleeper [34].

Fig. 2b shows variations in the normalized energy, E_n, at their current average seat occupancy levels. Bus&coach and high-speed train have a moderate and high capacity, respectively. They are the most energy-efficient ones with low normalized energies ranging from 0.15 to 0.73 MJ/(person·km). The seat capacities for aircraft locate between bus&coach and high-speed train, while their E_n values are around 2—3 times higher than those of high-speed train and bus&coach, ranging from 0.94 to 1.74 MJ/(person·km). For automobile, it has the widest range from 0.31 to 2.53 MJ/(person·km) due to different fuel types. Electric/hybrid automobiles (grey triangles) are generally more energy efficient with low E_n values (≤1.10 MJ/(person·km)) compared to those of diesel and petrol automobiles. It may be noted that at the current seat occupancy level (i.e. $\alpha = 0.32$), the E_n values of some automobiles are even higher than those of aircraft, making these automobiles the least energy-efficient transportation modes. However, if pushing the automobile seat usage level to its maximum ($\alpha=1$), their E_n values could be reduced to <0.81 MJ/(person·km) and became comparable to that of buses and high-speed trains. This indicates the energy efficiency of automobiles can be significantly improved by increasing their seat usage. One realistic example is the ride-sharing that we use in our daily lives. Overall, electrically driven vehicles, i.e. electrical cars, some buses and high-speed trains, consume normalized energy below 1.10 MJ/(person·km), which is less than those of fuel-driven vehicles, up to 2.53 MJ/(person·km), and are more recommended for travelling.
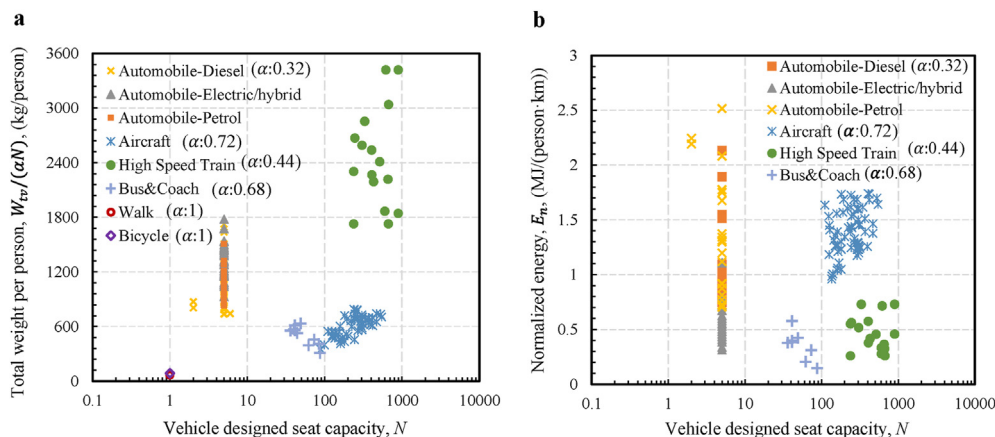

Fig. 2. Variations in $W_{tv}/(\alpha N)$ and E_n for different vehicle types at their current average seat occupancy levels. **a**, $W_{tv}/(\alpha N)$ for each vehicle type. **b**, E_n for each vehicle type. Note that 'α' represents the current average occupancy level for each vehicle type.
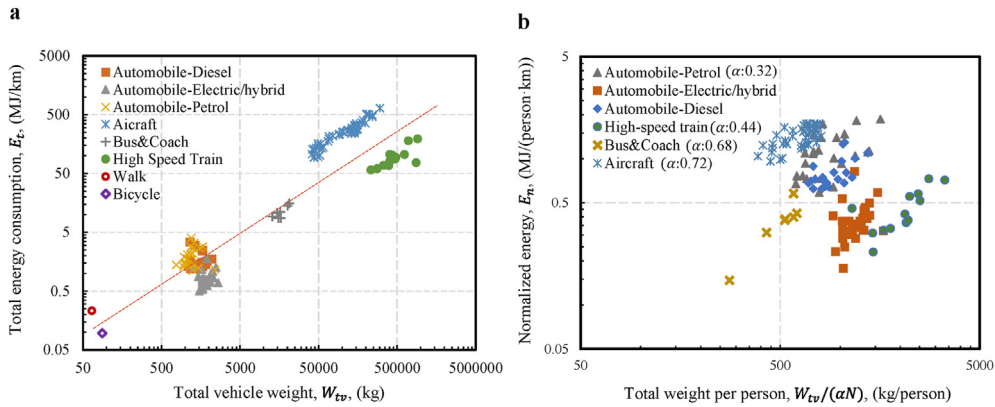
Fig. 3. Relation of energy consumption to weight. **a**, Energy consumption vs. total vehicle weight. **b**, E_n vs. $W_{tv}/(\alpha N)$ considers the average occupancy level, α, for each vehicle type.

3. Energy to weight relations

Relations between energy and weight are shown in Fig. 3. This illustrates the benefit of achieving reduced energy consumption by reducing vehicle weight. For energy vs. total weight in Fig. 3a, heavier vehicles consume more energy per km travelling for individual vehicle types, and all plotted points can be approximated to a linear relation on a log-log scale. High-speed trains and aircraft locate at the top-right corner and are the heaviest among other transportation types with their total weight ranging from ~200 t to ~900 t and ~37 t to ~280 t, respectively, based on the collected data set. The total energy consumptions are also high, up to 643 MJ/km for aircraft and 242 MJ/km for the high-speed train. Though the total energy consumption of aircraft is around 10 times higher than that of the high-speed train at a same weight level, they both follow linear relations. The automobiles present at the bottom left region with their total weights around 730−2600 kg and total energy consumption around 0.5−4.0 MJ/km, according to the mile per gallon (mpg) values based on their specifications. Though the data is a bit crowded, it can still be seen that the total energy consumptions increase with the total weights for different fuel types. Bus&coach stays in the middle region with a total weight of around 12 t to 18 t. In general, points for electrical driven vehicles (i.e. automobiles-electric and high-speed trains) are slightly lower than the average line while those for fuel-driven vehicles are slightly higher, indicating better energy efficiency for electrical driven vehicles.

The normalized energy vs. total weight per person at their current occupancy level is plotted in Fig. 3b. Most transportation

modes experience normalized energy of 0.2−1.8 MJ/(person·km). Bus&coach, automobile-electric and high-speed train are more energy-efficient than others at their current average occupancy level, α, with most of the E_n values are below 0.5 MJ/(person·km). Although the points for E_n vs. $W_{tv}/(\alpha N)$ relation are crowded, it can still be perceived that normalized energy increases with $W_{tv}/(\alpha N)$ value for each transportation type.

4. Methodology of the vehicle mass index development

This section focused on the development of the VMI, which is inspired by the BMI. The key aspects of BMI are: (i) body fat percentage is a metric for evaluating human health level. (ii) BMI relates linearly to body fat percentage so that important conditions are readily identified by the index. For instance, a body fat ranging between 18% and 25% in men and 25% and 32% in women translate to BMI of <18.49 underweight and ≥25 overweight for both women and men (Word heath organization, 1995). This is shown graphically in Fig. 4. Linear relationships vary for different age and gender groups [32,35]. (iii) BMI is a function of weight and height. Hence, using two easily measured dimensions, a BMI value is obtained to indicate health level. The world health organization (WHO) standard equation is [30], $BMI = \frac{weight\ (kg)}{height^2\ (m^2)}$.

Similar considerations were employed in constructing VMI as follows: (i) The purpose is to provide a universal means for evaluating energy efficiency of any mass transport vehicle. The normalized energy, which is the energy required per passenger for travelling 1 km is taken as the metric for evaluating efficiency. (ii)
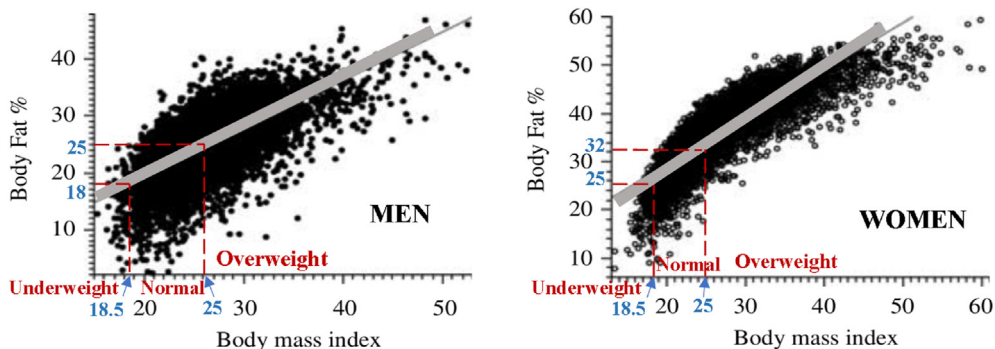

Fig. 4. Correlation between body fat percent and BMI [35]. Underweight with *BMI* < 18.49, normal weight with *BMI* in the range of 18.50−24.99, overweight with *BMI* ≥ 25.00 for both men and women [30].

VMI shall relate linearly to the normalized energy to enable energy efficiency to be identified by the index. Besides, VMI shall enable one linear relationship for all vehicle types, providing a means for their global comparison. (iii) VMI should be a function of easily measured key parameters. Knowing that energy consumption is related to total vehicle weight, VMI is then defined as a function of total vehicle weight, total seat capacity and the occupancy level, which are three easily measured key features based on the design and the use of the vehicle.

A normalized weight, R, which is defined as the ratio of total vehicle weight, W_{tv}, divided by the total passenger weight, W_{tp}, is

$$R = \frac{W_{tv}}{W_{tp}} = \frac{W_c + \alpha N \cdot W_p}{aN \cdot W_p} \tag{3}$$

where $\alpha = 1$ means the fully loaded condition.

Plotting normalized energy, E_n, against the normalized weight, R, on a log-log scale (Fig. 5) with the consideration of their current average occupancy levels, a linear relation is identified for each vehicle type, which can be approximated by the expression:

$$E_n = AR^n \tag{4}$$

where $R \geq 1$. $R = 1$ represents a theoretically weightless vehicle. The slope of each best fit line, n, is the weight sensitivity exponent and is related to the power efficiency of a vehicle at the given occupancy level. A high value indicates that energy consumption increases significantly with weight increase. $n = 0$ is not possible as weight always affects energy consumption in practice. Intercept A (where $R = 1$) is related to the minimum energy efficiency of the theoretically weightless vehicle for each vehicle type at the given occupancy level.

Values of n and A extracted from the best fittings in Fig. 5 with the consideration of current average occupancy level for each vehicle type are listed in Table 1 n and A values for $\alpha = 1$ are also determined using the same method from the best fittings of E_n vs. R plot, and the values are also provided in Table 1 in brackets. Overall, land vehicles have higher n values but lower A values than that of aircraft. This indicates the reduction in energy consumption for land vehicles is more sensitive to weight reduction, while and the energy consumption is less than that of aircraft for a given

normalized weight. The lowest n value for aircraft indicates its lowest energy sensitivity to the weight change, while its highest A value shows that the highest normalized energy is consumed for a given normalized weight.

Based on the above analysis, the Vehicle Mass Index, I, is defined as:

$$I = AR^n \tag{5}$$

where I equals E_n. Plotting E_n vs. I using the determined n and A values for the current average occupancy level in Table 1 gives a single linear relationship for all vehicle types with the consideration of occupation level, as shown in Fig. 6. The correlation coefficient to linearity is 0.86, indicating acceptable fitting.

Normalized energy can be seen to increase with I values for all transportation types. Electric driven automobiles, high-speed trains and bus & coach are located at the bottom left corner with low I and E_n values, indicating better energy efficiency, while aircraft are located at the top right corner with high I values. Automobiles-petrol and -diesel spread in the middle ranges. Using the vehicle mass index, the normalized energy can be directly evaluated from vehicle weight, seat capacity and occupancy levels. Such index also enables direct comparison of the energy efficiency between different transportation types using the determined corresponding A and n values.

5. Evaluation of the lower boundary of I for automobiles at the current average occupancy level

In this section, a method for determining the VMI for the minimum possible weight for a real-world automobile is developed. A practically acceptable automobile has three critical stability characteristics: (i) controllable acceleration and braking, (ii) controllable cornering and (iii) crosswind stability [36]. Reducing automobile mass increases achievable braking and acceleration rate [37,38] and cornering velocity [39]. Therefore, characteristic (iii) is focused on examining the minimum weight necessary to obviate either rollover or slip in a crosswind.

According to the Lateral Load Transfer Ratio method [40], the threshold value for rollover is expressed in Eqn. (6)

$$LLTR = \frac{|N_1 - N_2|}{N_1 + N_2} \in [0, 1] \tag{6}$$

where N_1 and N_2 denote vertical supporting forces on the left and right supporting wheels.

An LLTR value of 1 indicates the critical state for rollover, where one of the supporting forces equals 0. N_1 and $N_2 \geq 0$ are the boundary conditions to prevent rollover. From stress and moment analysis under windy conditions [41], the weight criteria to prevent rollover have been determined in Eqn. (7). The boundary condition to prevent slip under windy conditions is related to whether the friction force can resist the resultant of wind and centrifugal force. The weight criteria to prevent slip is given in Eqn. (8). The detailed analysis is provided in Appendix B.

$$\text{Prevent Rollover } W_{tv} \geq \frac{C_s \rho v_{wind}^2 S}{2\left(\frac{B}{2h}g - \frac{v^2}{r}\right)} \tag{7}$$

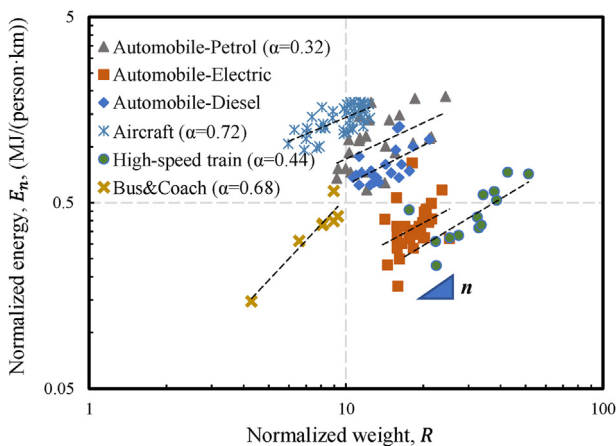$$\text{Prevent Slip } W_{tv} \geq \frac{C_s \rho v_{wind}^2 S}{2\left(\mu g - \frac{v^2}{r}\right)} \tag{8}$$

Fig. 5. Normalized energy, E_n, vs. normalized weight, R, with the consideration of the current average occupancy level, α, for each vehicle type. The α value for each vehicle is given in the figure legend. The normalized energy approximately linearly increases with the normalized weight for each vehicle type on the log-log scales. The dash lines are the best fittings for each type and the slope, n, presents the sensitivity of the weight on the normalized energy.

Table 1
The determined weight sensitivity exponent, n, and the energy efficiency constant, A, for different vehicle types with the consideration of their current average occupancy levels. The values in the brackets indicating the values determined with $\alpha = 1$, i.e. the designed full seat capacity of the vehicles.

	Automobile-Petrol	Automobile-Diesel	Automobile-Electrical	Bus & Coach	High-Speed Train	Aircraft
n (−)	0.71	0.71	0.74	1.47	0.83	0.57
	(0.74)	(0.82)	(0.82)	(1.62)	(0.87)	(0.60)
A (MJ/(person·km))	0.17	0.12	0.04	0.02	0.02	0.39
	(0.10)	(0.07)	(0.03)	(1.50e-3)	(1.84e-3)	(0.31)
Current average occupancy level	0.32	0.32	0.32	0.68	0.44	0.72

C_s (=1.90 [42] for cars) is the aerodynamic coefficient, ρ (=1.225 kg/m³) the air density, v_{wind} (=17.2 m/s, windy level 8) the wind velocity, S the projected area normal to the wind force, B the

Fig. 6. Relation between normalized energy, E_n, and vehicle mass index, I, at the current average occupancy level for six vehicle types. The dashed line presents a 1:1 increase in the normalized energy with the vehicle mass index. I values are calculated using the curb weights, the corresponding average occupancy level, and the determined A and n values in Table 1.

width between two wheels and h the centroid height, v the automobile velocity, r the cornering radius, g (=9.80 m/s²) the gravity acceleration, μ (=0.50 for dry asphalt) the friction coefficient between tyres and road.

The Toyota RAV4 (Petrol) with a curb weight of 2130 kg is used as a case study. Dimensions and weight of Toyota RAV4 were taken from Toyota RAV4 specification [43], and the projected area of the Toyota RAV4 was estimated as $\frac{3}{4}$·height·weight. Relevant dimensions are $S = 5.81$ m², $B = 1.86$ m and $h = 0.56$ m. Taking straight driving (r=infinity) at the average occupancy level as the case study, calculation shows: $W_c \geq 304\ kg$ to prevent slip, and $W_c \geq 20\ kg$ to prevent rollover. Therefore, the lower curb weight limit is 304 kg, which is much less than the current curb weight of 2130 kg of the vehicle. This indicates that neglecting other factors, the car could be much lighter whilst remaining drivable. Substituting $W_c = 304\ kg$ into *VMI* yields $I_{min} = 0.45$. Compared with the current I value of 1.46, there is a huge potential for weight reduction of the vehicle to reduce energy usage.
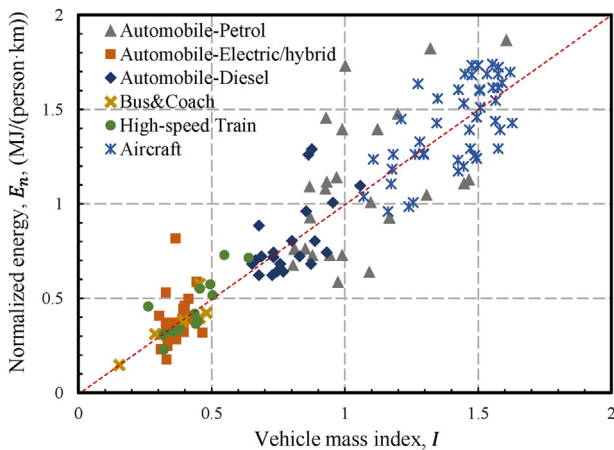
6. Results and discussion

Fig. 7 provides an overall summary of the determined VMI for the analysed vehicle types. Fig. 7a shows VMI ranges for various transportation types at their current average occupancy levels. Overall, the investigated I values range from 0.15 to 1.62 with lower VMI representing greater energy efficiency. Electrically-driven vehicles
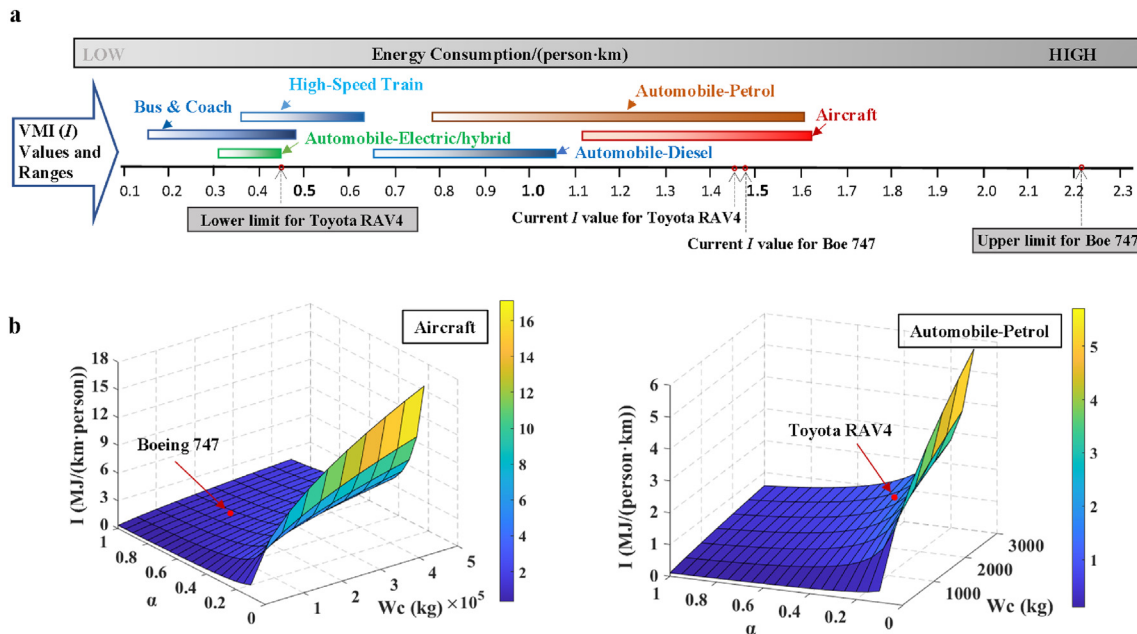

Fig. 7. Vehicle mass index, I, values for various vehicle types. **a**, Ranges of vehicle mass index for the analysed vehicle types at their current occupancy levels. Aircraft Boe 747 and automobile Toyota RAV4 are taken as two examples to show their current I values and possible limits on the scale. **b**, Relations of I to vehicle curb weight, W_c, and occupancy level α, for aircraft and automobile-petrol. Note that the I values are calculated using Eqn. (5) with the determined A and n values for the corresponding occupancy levels.

have lower VMI values compared with fuel-driven vehicles. Aircraft and some automobile-petrol models are the least energy-efficient ways for travelling, while buses and coaches have the highest energy efficiency at their current occupancy levels. Taking automobile-diesel as an example, I ranges from 0.65 to 1.06 and the corresponding curb weight range is 1005 kg–2090 kg. Such large weight disparity in current passenger diesel cars indicates a significant window exists for weight reduction to increase energy efficiency.

The calculated lower bound value of I at the current average occupancy level for the Toyota RAV4 (Automobile-petrol) is 0.45 with the corresponding curb weight of 304 kg, while the current model has an I value of 1.46 and 2130 kg curb weight. This example is annotated on Fig. 7a and indicates an existing large window of opportunity for reducing automobile weights before reaching their VMI lower limits if physically possible. There is no lower limit of VMI value for aircraft, but an upper limit exists based on take-off thrust-to-weight ratio. Boeing 747 was used as an example to show its upper limit (i.e. 2.22) and current I value (i.e.1.48) in Fig. 7a, corresponding to its operation empty weight (i.e.183.5 t) and the maximum take-off weight (i.e.396.9 t).

Fig. 7b presents the effects of the curb weight and occupancy levels on the I values, and hence energy efficiencies, for aircraft and automobile-petrol based on equation (5) and the corresponding A and n values extracted from the collected data. Locations for the current Boeing 747 and Toyota RAV4 are also highlighted in the figure. Values for both aircraft and automobile-petrol follow the same trend, where the normalized energy shows an exponential increase with the increase in vehicle curb weights and the decrease in the occupancy level. It can be seen that the way to increase energy efficiency is to reduce the vehicle curb weight, increase their seat capacity and occupancy level. The locations of the Boeing 747 and Toyota RAV4 indicate there are still spaces to reduce the current weight and increase the occupancy rates to further push the I value down to their physically possible lower limits. When α equals 1, the I value could also be used to assess the fundamental energy efficiency of a particular vehicle, relating to their designed properties (i.e. weight and designed full seat capacity).

The proposed new VMI concept can be used to evaluate normalized energy for different transportation types, which will be critical to assess environmental compatibility and identify green-compliant transport modes for the 'zero-emissions' future. The idealised limits of VMI also provide clear targets which can be approached by weight reduction, increasing the seat capacity and seat usage. International statistics could be made widely available to aid customer purchasing, using, and motivating competition among manufacturers to reduce their VMI values.

7. Conclusions and policy implications

A universal vehicle mass index (VMI) has been proposed, to assess the energy efficiency of different types of passenger vehicles based on weight, seat capacity and current levels of passenger occupancy. Statistical analysis of weight, seat capacity, energy consumption and occupancy level are performed for automobiles, bus & coaches, high-speed trains and aircraft. Such index, for the first time, locates all transportation types on a unified scale and enables global comparison of the energy efficiencies between different transportations. Specific conclusions are:

(i) An appropriate definition of VMI has been found to be, $I = A\left(\frac{W_{tv}}{W_{tp}}\right)^n$, where W_{tv} is the total vehicle weight (including the passenger weight), W_{tp} is the total passenger weight, A is the energy efficiency of a theoretically weightless vehicle and n

is the weight sensitivity parameter. Aircraft have the highest vehicle mass index I values, up to 1.62, while bus& coaches have the lowest values, with a minimum of 0.15, at their current average occupancy levels.

(ii) The I value and normalized energy decrease exponentially with the reduction in vehicle curb weight and the increase in occupancy level. For diesel automobiles, I ranges from 0.65 to 1.06 corresponding to a curb weight of 1005–2092 kg, respectively. A significant window to reduce energy consumption through weight reduction is apparent.

(iii) An assessment of the upper and lower boundaries for the VMI from simple dynamics analysis shows, in theory, I value for the automobile Toyota RAV4 could be reduced from its current value of 1.46 to 0.45. This would lead to 70% energy saving on the road. Calculation for the Boeing 747 for example gives its current I value as 1.48 and the upper limit as 2.22.

(iv) Aircraft have the highest value of energy efficiency parameter A (0.39 MJ/(person·km)) and lowest energy sensitivity value n (0.57). The energy efficiency of land transportation is more sensitive to weight reduction with higher n values (>0.7).

Further work is required to increase data for deriving A and n data used for evaluating VMI values for all types of human vehicles at various driving conditions and to define their theoretically possible lowest limits of curb weight. The theory supporting the VMI concept could also be applied or adapted for energy efficiency assessment and form the basis of a worldwide standard useful in the current drive for a greener economy and zero CO_2 emissions in the near future. Scientists and engineers in relevant fields are encouraged to improve on this version and provide more comprehensive data to develop it as an international standard for energy efficiency assessment for different types of vehicles.

Conflicts of interest

The authors declare that there is no conflicts of interest.

Acknowledgements

Appendix A

Data collection and analysis.

Curb weight, designed seat capacity and energy data for automobile, bus/coach, aircraft and high-speed train were collected from the vehicle certification agency [44], published specifications [45–52], leasing company specifications, public reports and manuals [53–70]. Energy consumption of hydrocarbon fueled automobiles and aircraft was calculated by multiplying, fuel consumption by its energy density, litre/km × MJ/litre. Energy densities [71] were petrol (34.2 MJ/L), diesel (38.6 MJ/L) and kerosene (37.4 MJ/L). Bus/coach and high-speed train energy consumption were obtained from electrical power consumption (Kwh) and converted to Mega Joules (MJ). The energy data for walking and

cycling were taken from calories burned [72] at a walking and cycling speed of 6 km/h and 16 km/h, respectively.

Appendix B

VMI lower boundary determination of automobile stability

The Lateral Load Transfer Ratio (LLTR) method [73] was used to estimate the minimum weight without slip and rollover. According to LLTR method, the threshold value for rollover is expressed in Eqn (A-1)

$$LLTR = \frac{|N_1 - N_2|}{N_1 + N_2} \in [0, 1] \tag{A-1}$$

where N_1 and N_2 denote the supporting forces on the wheels as schematically illustrated in A1. LLTR equal to 1 indicates the critical state for rollover, where one of the supporting forces equals 0. LLTR equals to 0 indicate the stable state, where $N_1 = N_2$.
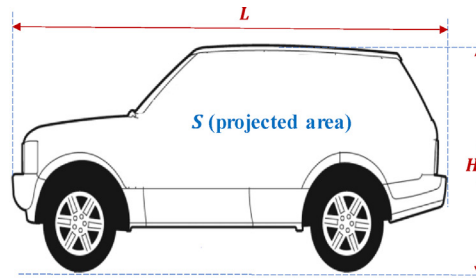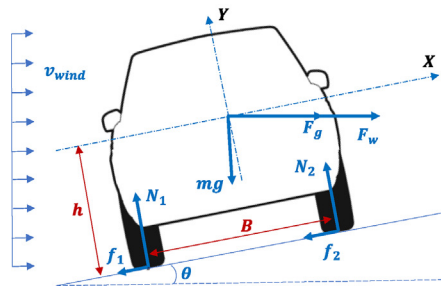

Fig. A1. Stress analysis on an automobile.

Consider a general case, where a vehicle was driving on a road with a tilt angle of $\theta \geq 0°$. $\theta = 0°$ means the vehicle is driving on a horizontal road. Then stress analysis was performed as shown in Fig. A1. The vertical supporting forces N_1, N_2 and friction forces f_1, f_2 could be calculated from force and moment balances, as presented in Eqn. (A-2, A-3, A-4),

$$N_1 = \frac{mg}{2}cos\theta + \frac{(F_g + F_w)}{2}sin\theta + \frac{mgh}{B}sin\theta - \frac{(F_g + F_w)h}{B}cos\theta \tag{A-2}$$

$$N_2 = \frac{mg}{2}cos\theta + \frac{(F_g + F_w)}{2}sin\theta - \frac{mgh}{B}sin\theta + \frac{(F_g + F_w)h}{B}cos\theta \tag{A-3}$$

$$f = f_1 + f_2 = (F_g + F_w)\,cos\theta - mg\,sin\theta \tag{A-4}$$

where total weight (mg) in N, centrifugal force (F_g), wind force (F_w), tilt angle (θ), wind speed (v_w), wind projected area (S), centroid height (h), width (B), length (L) and total height (H) are illustrated in Fig. A1.

The wind force (F_w), centrifugal force (F_g) and friction force (f) could be attained from Eqn. (A-5, A-6, A-7) [73–75],

$$F_w = \frac{1}{2}C_s\rho v_{wind}^2 S \tag{A-5}$$

$$F_g = \frac{mv^2}{r} \tag{A-6}$$

$$f = \mu mg \tag{A-7}$$

where C_s is the aerodynamic coefficient, ρ the air density, v_{wind} the velocity of the wind, S the projected area normal to the wind force, v the automobile velocity, r the cornering radius, μ the friction coefficient, g the gravity acceleration. Slip occurs when $f \leq (F_g + F_w)\,cos\theta - mg\,sin\theta$ and rollover occurs when $N_1 = 0$. When driving on a horizontal road with $\theta = 0°$, which is the normal case, slip and rollover criteria could be achieved by substituting Eqn. (A-5, A-6, A-7) into Eqn. (A-2) and (A-4), yields

$$\text{Prevent Slip } m \geq \frac{C_s\rho v_{wind}^2 S}{2\left(\mu g - \frac{v^2}{r}\right)} \tag{A-8}$$

$$\text{Prevent Rollover } m \geq \frac{C_s\rho v_{wind}^2 S}{2\left(\frac{B}{2h}g - \frac{v^2}{r}\right)} \tag{A-9}$$

Note that m is the total vehicle weight in kg, equals to W_{tv}.

References

[1] I. Meyer, S. Wessely, Fuel efficiency of the Austrian passenger vehicle fleet-Analysis of trends in the technological profile and related impacts on CO2 emissions, Energy Pol. 37 (2009) 3779–3789, https://doi.org/10.1016/j.enpol.2009.07.011.

[2] D.L. Mccollum, W. Charlie, B. Michela, C. Samuel, O.Y. Edelenbosch, E. Johannes, G. Céline, K. Panagiotis, K. Ilkka, K. Volker, Interaction of consumer preferences and climate policies in the global transition to low-carbon vehicles, Nat. Energy 3 (2018) 664–673, https://doi.org/10.1038/s41560-018-0195-z.

[3] D.L. Greene, C.B. Sims, M. Muratori, Two trillion gallons: fuel savings from fuel economy improvements to US light-duty vehicles, 1975-2018, Energy Pol. 142 (2020) 111517, https://doi.org/10.1016/j.enpol.2020.111517.

[4] D.V. Wagner, F. An, W. Cheng, Structure and impacts of fuel economy standards for passenger cars in China, Energy Pol. 37 (2009) 3803–3811, https://doi.org/10.1016/j.enpol.2009.07.009.

[5] L. Zhu, N. Li, P.R.N. Childs, Light-weighting in aerospace component and system design, Propul. Power Res. 7 (2018) 103–119, https://doi.org/10.1016/j.jppr.2018.04.001.

[6] A.P. Moneo, Analysis of technological and competitive trends of weight reduction in high speed rolling stock industry, Proyecto Fin de Carrera/Trabajo Fin de Grado, E.T.S.I. Industriales (UPM), 2016.

[7] M. Marino, R. Sabatini, Advanced lightweight aircraft design configurations for green operations, in: Proceedings of the Practical Responses to Climate Change 2014 (PRCC 2014), 2014, https://doi.org/10.13140/2.1.4231.8405.

[8] N.P. Lutsey, Review of Technical Literature and Trends Related to Automobile Mass-Reduction Technology, Institute of Transportation Studies, University of California, Davis, 2010.

[9] F. Chiara, M. Canova, A review of energy consumption, management, and recovery in automotive systems, with considerations of future trends, Proc.

Inst. Mech. Eng. - Part D J. Automob. Eng. 227 (2013) 914–936, https://doi.org/10.1177/0954407012471294.

[10] C.A. Kennedy, A comparison of the sustainability of public and private transportation systems: study of the Greater Toronto Area, Transportation 29 (2002) 459–493, https://doi.org/10.1023/A:1016302913909.

[11] K. Hu, Y. Chen, Technological growth of fuel efficiency in european automobile market 1975-2015, Energy Pol. 98 (2016) 142–148, https://doi.org/10.1016/j.enpol.2016.08.024.

[12] U.L. Hinrich Helms, Hopfner Ulrich, Energy Savings by Light-Weighting Final Report, IFEU-Institut fur Energie und Umweltforschung Heidelberg GmbH, 2003.

[13] H. Liimatainen, M. Poellaenen, Trends of energy efficiency in Finnish road freight transport 1995-2009 and forecast to 2016, Energy Pol. 38 (2010) 7676–7686, https://doi.org/10.1016/j.enpol.2010.08.010.

[14] H. Jung, R. Silva, M. Han, Scaling trends of electric vehicle performance: driving range, fuel economy, peak power output, and temperature effect, World Elect. Veh. J. 9 (2018) 46, https://doi.org/10.3390/wevj9040046.

[15] M.S. Mohamed, A.D. Foster, J. Lin, D.S. Balint, T.A. Dean, Investigation of deformation and failure features in hot stamping of AA6082: experimentation and modelling, Int. J. Mach. Tool Manufact. 53 (2012) 27–38, https://doi.org/10.1016/j.ijmachtools.2011.07.005.

[16] W. Zhou, J. Lin, T.A. Dean, L. Wang, Analysis and modelling of a novel process for extruding curved metal alloy profiles, Int. J. Mech. Sci. 138e139 (2018) 524–536, https://doi.org/10.1016/j.ijmecsci.2018.02.028.

[17] D.J. Politis, J. Lin, T.A. Dean, D.S. Balint, An investigation into the forging of Bi-metal gears, J. Mater. Process. Technol. 214 (2014) 2248–2260, https://doi.org/10.1016/j.jmatprotec.2014.04.020.

[18] K. Zheng, Y. Dong, D. Zheng, J. Lin, T.A. Dean, An experimental investigation on the deformation and post-formed strength of heat-treatable aluminium alloys using different elevated temperature forming processes, J. Mater. Process. Technol. 268 (2018) 87–96, https://doi.org/10.1016/j.jmatprotec.2018.11.042.

[19] M. Janic, High-speed rail and air passenger transport: a comparison of the operational environmental performance, Proc. Inst. Mech. Eng. - Part F J. Rail Rapid Transit 217 (2003) 259–269, https://doi.org/10.1243/095440903322712865.

[20] P.J. Perez-Martinez, I.A. Sorba, Energy consumption of passenger land transport modes, Energy Environ. 21 (2010) 577–600, https://doi.org/10.1260/0958-305X.21.6.577.

[21] S. Das, D. Graziano, V. Upadhyayula, E. Masanet, M. Riddle, J. Cresko, Vehicle lightweighting energy use impacts in U.S. light-duty vehicle fleet, Sustain. Mater. Technol. 8 (2016) 5–13, https://doi.org/10.1016/j.susmat.2016.04.001.

[22] A. Kharina, D. Rutherford, Fuel Efficiency Trends for New Commercial Jet Aircraft: 1960 to 2014, The International Council on Clean Transportation, 2015.

[23] The World Bank, Air transport and energy efficiency. https://documents.worldbank.org/en/publication/documents-reports/documentdetail/746271468184153529/air-transport-and-energy-efficiency, 2012. (Accessed 11 June 2021).

[24] J. Hofer, E. Wilhelm, W. Schenler, Comparing the mass, energy, and cost effects of lightweighting in conventional and electric passenger vehicles, J. Sustain. Dev. Energy Water Environ. Syst. 2 (2014) 284–295, https://doi.org/10.13044/j.sdewes.2014.02.0023.

[25] A.T. Mayyas, A. Qattawi, A.R. Mayyas, M.A. Omar, Life cycle assessment-based selection for a sustainable lightweight body-in-white design, Energy 39 (2012) 412–425, https://doi.org/10.1016/j.energy.2011.12.033.

[26] J.J. Lee, S.P. Lukachko, I.A. Waitz, A. Schafer, Historical and future trends in aircraft performance, cost, and emissions, Annu. Rev. Energy Environ. 26 (2001) 167–200, https://doi.org/10.1146/annurev.energy.26.1.167.

[27] International Civil Aviation Organization, Aircraft CO2 emission standard metric system. http://www.icao.int/environmental-protection/Documents/CO2%20Metric%20System%20-%20Information%20Sheet.pdf, 2013. (Accessed 11 June 2021).

[28] International Council on Clean Transportation, International civil aviation organization's CO2 certification requirement for new aircraft. https://theicct.org/sites/default/files/publications/ICCTupdate_ICAO_CO2cert_aug2013a.pdf, 2013. (Accessed 11 June 2021).

[29] International Council on Clean Transportation, International civil aviation organization's CO2 standard for new aircraft. https://theicct.org/sites/default/files/publications/ICCT-ICAO_policy-update_revised_jan2017.pdf, 2017. (Accessed 11 June 2021).

[30] W. E. C. o. P. Status, Physical status: the use and interpretation of anthropometry, 1995. Geneva, Switzerland.

[31] F.Q. Nuttall, Body mass index: obesity, BMI, and health: a critical review, Nutr. Today 50 (2015) 117–128, https://doi.org/10.1097/NT.0000000000000092.

[32] A. Keys, F. Fidanza, M.J. Karvonen, N. Kimura, H.L. Taylor, Indices of relative weight and obesity, J. Chron. Dis. 25 (1972) 329–343, https://doi.org/10.1016/0021-9681(72)90027-6.

[33] European Environment Agency, Occupancy rates of passenger vehicles. https://www.eea.europa.eu/data-and-maps/indicators/occupancy-rates-of-passenger-vehicles/occupancy-rates-of-passenger-vehicles, 2015. (Accessed 11 June 2021).

[34] ZEFIRO-Brochure, Zefiro: a new sense of speed. http://craston.de/wp-content/uploads/ZEFIRO-Brochure.pdf, 2009. (Accessed 11 June 2021).

[35] A. Romero-Corral, V.K. Somers, J. Sierra-Johnson, R.J. Thomas, M.L. Collazo-Clavell, J. Korinek, T.G. Allison, J.A. Batsis, F.H. Sert-Kuniyoshi, F. Lopez-Jimenez, Accuracy of body mass index in diagnosing obesity in the adult general population, Int. J. Obes. 32 (2008) 959–966, https://doi.org/10.1038/ijo.2008.11.

[36] T.D. Gillespie, Fundamentals of Vehicle Dynamics, Society of Automotive Engineers, Warrendale, PA, 1992.

[37] A. Schallamach, The load dependence of rubber friction, Proc. Phys. Soc. London, Sect. B 65 (1952) 657–661, https://doi.org/10.1088/0370-1301/65/9/301.

[38] V. Dorsch, A. Becker, L. Vossen, Enhanced rubber friction model for finite element simulations of rolling tyres, Plast. Rubber Compos. 31 (2002) 458–464, https://doi.org/10.1179/146580102225006486.

[39] M. Abe, Vehicle Handling Dynamics, second ed., Butterworth-Heinemann, Oxford, 2015.

[40] D. Xiao, H. Duan, M. Wang, Research on operation safety of windy area on highway based on lateral stability, Highways 4 (2017), 0168.

[41] B. Abdessalem, Methods of calculating aerodynamic force on a vehicle subject to turbulent crosswinds, Am. J. Fluid Dynam. 3 (2013) 119–134, https://doi.org/10.5923/j.ajfd.20130304.04.

[42] C.J. Baker, Measures to control vehicle movement at exposed sites during windy periods, J. Wind Eng. Ind. Aerod. 25 (1987) 151–161, https://doi.org/10.1016/0167-6105(87)90013-4.

[43] Toyota RAV4 specification. https://www.toyota.co.uk/new-cars/rav4/features-and-specs, 1995. (Accessed 11 June 2021).

[44] Vehicle certification agency, New car fuel consumption& emission figures, 2018. https://carfueldata.vehicle-certification-agency.gov.uk/additional/sept2018/BD003 Rev 8 Fuel Consumption Guide - Final text1.pdf. (Accessed 10 May 2021).

[45] Ford specifications, 2021. https://www.ford.co.uk/cars/new-fiesta/models-specs/trend. (Accessed 10 May 2021).

[46] available from:, Citroen vehicle specification, 2021 https://www.citroen.co.uk/new-cars-and-vans/citroen-range/citroen-c4-cactus/configurator/view-my-configuration/technical-specification. (Accessed 10 May 2021).

[47] available from:, Alexander dennis specifications, 2021 https://www.alexander-dennis.com/. (Accessed 10 May 2021).

[48] available from:, Optare specification, 2021 optare.com/metrocity. (Accessed 10 May 2021).

[49] available from:, Nissan specification, 2018 https://en.nissanqatar.com/vehicles/new/x-trail/specifications.html. (Accessed 10 May 2021).

[50] available from:, Toyota corolla e-brochure, 2019 https://www.toyota.com/corolla/ebrochure/. (Accessed 10 May 2021).

[51] available from:, Bombardier CRJ1000 specifications. FlyRadius, 2015 https://www.flyradius.com/bombardier-crj1000/specifications. (Accessed 10 May 2021).

[52] Chris Brady, The boeing 737 technical site, available from:, 2010 http://www.b737.org.uk/techspecsdetailed.htm. (Accessed 10 May 2021).

[53] available from:, Electric vehicle database, 2021 https://ev-database.uk/. (Accessed 10 May 2021).

[54] Audi A2: 1999, World's first volume-production alumnium car, Available from:, 1999 https://cartype.com/pages/866/audi_a2__1999. (Accessed 10 May 2021).

[55] available from:, Fuel economy in aircraft, 2021 https://en.wikipedia.org/wiki/Fuel_economy_in_aircraft. (Accessed 10 May 2021).

[56] Aircraft Commerce, CRJ family fuel-burn performance, available from:, 2009 http://www.team.aero/files/aviation_data/owners_n_operators_guide_crj.pdf. (Accessed 10 May 2021).

[57] available from:, Aircraft Commerce, Owner's & Operator's guide: E-Jets family, 2009 http://www.team.aero/files/aviation_data/owners_n_operators_guide_e_jets.pdf. (Accessed 10 May 2021).

[58] Bombardier Commercial Aicraft, Environmental product declaration, available from:, 2016 https://gryphon4.environdec.com/system/data/files/6/12107/epd921_Bombardier_C_SERIES100.pdf. (Accessed 10 May 2021).

[59] Bombardier, Q400 fuel efficiency manual, available from:, 2014 https://www.scribd.com/document/359616493/Q400-Fuel-Efficiency-manual-pdf. (Accessed 10 May 2021).

[60] China CNR, CRC high speed train manufacturing strength presentation, available from:, 2010 https://web.archive.org/web/20130704164527/http://www.eng.ku.ac.th/blog/wp-content/uploads/rolling/16/CNR%20After.pdf. (Accessed 10 May 2021).

[61] available from:, CS300 First Flight Wednesday, Direct Challenge to 737-7 and A319neo, Leeham News, 2015 https://leehamnews.com/2015/02/25/cs300-first-flight-wednesday-direct-challenge-to-737-7-and-a319neo/. (Accessed 10 May 2021).

[62] FlyRadius, Bombardier CRJ1000 fuel consumption, available from:, 2013 https://www.flyradius.com/bombardier-crj1000/fuel-burn-fuel-consumption. (Accessed 10 May 2021).

[63] Pilatus, PC-12 NG just the facts, available from:, 2016 https://web.archive.org/web/20160211043621/http://www.pilatus-aircraft.com/00-def/main/scripts/ckfinder/userfiles/files/Downloads/Brochures/Pilatus-Aircraft-Ltd-PC-12NG-JustTheFacts.pdf. (Accessed 10 May 2021).

[64] Railway Gazette, Eurostar orders seven more e320s, available from:, 2014 https://www.railwaygazette.com/europe/eurostar-orders-seven-more-e320s/40210.article. (Accessed 10 May 2021).

[65] available from:, Robins & day, 2021 https://www.robinsandday.co.uk/. (Accessed 10 May 2021).

[66] available from:, Saab 2000 data sheet. Saab aircraft leasing, 2009 http://www.saabaircraftleasing.com/prod/datasheets/2000_JAR.pdf. (Accessed 10 May 2021).

[67] available from:, Saab 340A data sheet. Saab aircraft leasing, 2009 http://www.saabaircraftleasing.com/prod/dataSheets/340A_JAR.pdf. (Accessed 10 May 2021).

[68] available from:, SAAB aircraft leasing, specification, 2021 http://www.saabaircraftleasing.com/prod/downloads/. (Accessed 10 May 2021).

[69] available from:, Startup boeing, 2007 http://www.boeing.com/resources/boeingdotcom/company/about_bca/startup/pdf/historical/757_passenger.pdf. (Accessed 10 May 2021).

[70] 328 Support Services GmbH, Dornier 328-100 (TP), available from:, 2013 https://328.eu/wp-content/uploads/2013/06/328-100-turboprop.pdf. (Accessed 10 May 2021).

[71] K. Annamalai, I.K. Puri, Conbustion Science and Engineering, 2006.

[72] G. Chapman, Calories burned HQ, available from:, 2021 https://caloriesburnedhq.com/calorie-calculators/. (Accessed 10 May 2021).

[73] D. Xiao, H. Duan, M. Wang, Research on operation safety of windy area on highway based on lateral stability, Highways 4 (2017), 0168.

[74] B. Abdessalem, Methods of calculating aerodynamic force on a vehicle subject to turbulent crosswinds, Am. J. Fluid Dynam. 3 (2013) 119–134.

[75] A. Abdulwahab, Investigations on the Roll Stability of a Semitrailer Vehicle Subjected to Gusty Crosswind Aerodynamic Forces Doctoral Thesis, University of Huddersfield, 2018.